Selective transition to the closely-lying states Cs($7D_{3/2}$) and Cs($7D_{5/2}$) by femtosecond laser pulses

H. Yamada,[1,2] K. Yokoyama,[1,3,*] Y. Teranishi,[1] A. Sugita,[1] T. Shirai,[1] M. Aoyama,[1] Y. Akahane,[1] N. Inoue,[1] H. Ueda,[1] K. Yamakawa,[1] A. Yokoyama,[3] M. Kawasaki,[2] and H. Nakamura[4]

[1]*Advanced Photon Research Center, Japan Atomic Energy Research Institute, Kizu-cho, Kyoto 619-0215, Japan*

[2]*Graduate School of Global Environmental Studies, Kyoto University, Kyoto 615-8510, Japan*

[3]*Department of Materials Science, Japan Atomic Energy Research Institute, Tokai-mura, Ibaraki 319-1195, Japan*

[4]*Institute for Molecular Science, Myodaiji Okazaki, 444-8585, Japan*

(Received 20 June 2005; published 6 December 2005)

A demonstration of coherent quantum control for ultrafast precise selection of closely-lying states is reported. A phase-locked pair of femtosecond laser pulses is generated through a pulse shaper to excite the ground-state cesium atom to the Cs($7D_{3/2}$) and Cs($7D_{5/2}$) states by two-photon absorption. The excited state population is measured by detecting fluorescence from each spin-orbit state. By controlling the phase-difference of the pulse pair, an ultrafast precise selection is accomplished. The contrast ratio of the maximal to minimal selection ratio exceeds 10^3 with the delay less than 400 fs.

DOI: 10.1103/PhysRevA.72.063404 PACS number(s): 32.80.Qk

I. INTRODUCTION

Selection of quantum states by broadband lasers is of fundamental importance for the optical control of matter such as for laser isotope separation, laser manipulation of molecules, and chemical reaction control. The use of broadband lasers makes it possible to overcome various relaxation processes by taking advantage of their ultrafast character [1] and to provide an optimal laser field for complicated multistep selection processes owing to their polychromaticity [2]. However, the spectral broadness itself is harmful to precise selection. In other words, ultrafast and precise selections cannot be attained simultaneously with a simple transform limited (TL) pulse due to the uncertainty principle. To partially avoid this limitation, one can utilize the quantum interference of the wave function in the target states, i.e., quantum control. One of the aims of our study is to elucidate how fast and precisely state-selection can be made in a real system, using the state-of-the-art technique of pulse shaping as a powerful tool for quantum control [3].

We investigate a state-selective excitation of atoms into their closely-lying spin-orbit states. A few experiments have been reported so far for selecting spin-orbit states by a broadband laser [4–6]. Wefers and co-workers [5] demonstrated the selective excitation of potassium atoms to the K($4P_{1/2}$) and K($4P_{3/2}$) states via one-photon absorption around 770 nm, using a spatial light modulator (SLM). Because of the significant amount of background signal, the contrast ratio was relatively low, where the scattered light of the pump pulse and/or low spectral resolution in the state-resolved detection were pointed out as the limiting factors in measuring the populations. Blanchet and co-workers [6] showed clear modulation in the total excitation probability of two transitions of cesium atoms:

$$\mathrm{Cs}(7D_J \leftarrow 6S_{1/2}, J = 3/2 \text{ and } 5/2), \tag{1}$$

when they varied the delay between two pulses. Although they did not observe the individual spin-orbit state, the modulation implied that a temporally controlled pulse pair would selectively excite the spin-orbit states.

In this paper, we demonstrate the selection of spin-orbit states in transition (1) with an unprecedentedly high contrast ratio, by measuring the population of the individual state. The target states, Cs($7D_{3/2}$) and Cs($7D_{5/2}$), are produced by two-photon absorption of the ground state, Cs($6S_{1/2}$), at 767.82 and 767.20 nm, respectively. The final population of each excited state is measured by detecting the fluorescence from each state to the two different $6P$ states,

$$\mathrm{Cs}(7D_{3/2} \rightarrow 6P_{1/2}) \quad \text{at } 672.3 \text{ nm}, \tag{2}$$

$$\mathrm{Cs}(7D_{5/2} \rightarrow 6P_{3/2}) \quad \text{at } 697.3 \text{ nm}. \tag{3}$$

This scheme enables us to perform a well-resolved, extremely low background detection of each spin-orbit state without contamination of the pump light. The spin-orbit splitting between the Cs($7D_J$) states ($\Delta\omega = \omega_{5/2} - \omega_{3/2}$, 21 cm^{-1}) is much smaller than the bandwidth of the pump pulse ($\sim$380 cm^{-1}), so that both states would be simultaneously produced with ordinary unshaped pulses.

A key to achieve precise selection is making either one of the two states vanish. For this end we employ the same mechanism as the "Ramsey fringes" [5–8], using a phase-related pulse pair. In this mechanism, interference between wave functions created by the first and second pulses determines the final transition amplitude. In a fixed delay of pulse pair, by adjusting the phase-difference, we can wipe out the amplitude of either excited state in the weak field limit. When the amplitude of one excited state is perfectly wiped out, an exclusively selective excitation to the other state is realized.

*Email address: kei@apr.jaeri.go.jp

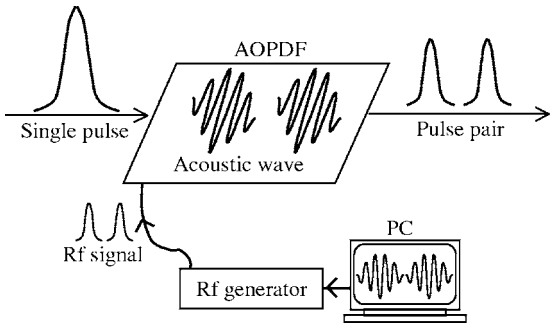

FIG. 1. Schematic of the generation of a pulse pair by the acousto-optic programmable dispersive filter (AOPDF). A pair of identical acoustic pulses is created in the TeO_2 crystal by the rf pulse pair, which is designed in a PC. From a single femtosecond optical pulse, a phase-related pulse pair is generated through the diffraction in the acoustic grating.

One of the important conditions to realize high selectivity through this mechanism is a sufficiently low peak intensity of the laser pulse. If the electric field is strong, the perturbative treatment is not valid any more and the amplitude of the excited state does not completely cancel out with two identical pulses. To simulate the observed selectivity, we theoretically examine the peak intensity dependence of the selectivity.

II. EXPERIMENT

The experimental apparatus consists of four components: a light source, a pulse shaper, a glass cell, and a detection system. The light source is a 82-MHz mode-locked Ti:sapphire laser without amplification systems and provides a femotosecond-pulse train without phase-relation among them. With the pulse shaper, a phase-related pulse pair is created from a single femtosecond pulse in the train. We employ Tournois's acousto-optic programmable dispersive filter (AOPDF; Fastlite, Dazzler) [9], which has no frequency gap unlike the SLM [10] and thus is expected to have the capability of precise pulse shaping [8]. To date, this device has been applied to few studies of quantum control [8,11] and thus the performance has not yet been well established. With this device, optical pulses are sculpted as follows: First, the waveform of rf electric pulses is shaped in the MHz region with a computer-controlled rf generator. Secondly, the rf electric pulse is converted to the acoustic pulse in the birefringent medium made of TeO_2 with the optical path length of 25 mm. Then, the acoustic pulse waveform is imprinted onto the incident optical pulse through the diffraction. Every incident optical frequency ω, initially polarized along the ordinary axis (mode 1), travels along the z axis and encounters a phase-matched spatial frequency in the acoustic grating. At this position $z(\omega)$, part of the energy is diffracted into mode 2 (along the extraordinary axis). Consequently, the optical output $E(\omega)$ is made of all the spectral components that have been diffracted at various positions according to the acoustic waveform. As shown in Fig. 1, a set of two identical acoustic waves outputs a pair of optical pulses from a single optical pulse. The two pulses in the pair are temporally separated, because the optical velocities of the two modes are different. The phase-difference of the pulse pair is specified through that of the acoustic waveform. The electric field $E(\omega)$ of the pulse pair is programmed as

$$E(\omega) = E_S(\omega) + E_S(\omega)\exp[i\{\tau(\omega - \omega_0) + \delta\Phi_0\}], \qquad (4)$$

where $E_S(\omega)$ is the frequency-domain electric field of a single pulse and nearly TL without explicit chirp, τ is the delay, $\delta\Phi_0$ is the phase-difference, and ω_0 is the center frequency of the single pulse. The group velocity dispersion of the TeO_2 crystal is compensated for by applying a linear chirp ($-13\,000$ fs^2) on the acoustic pulse. The acoustic pulse generated at 20 kHz travels from one end to the other of the crystal, taking ~ 23 μs, for which ~ 2000 optical pulses from the laser oscillator are modulated and transmitted by the crystal. It is to be noted that optical pulses are correctly shaped as designed only when the acoustic pulse stays in a proper range inside the TeO_2 crystal, and such correct pulses are about one tenth part of the transmitted pulses.

The programmable spectral window in the operation of the AOPDF was set to be 20 nm with the center wavelength of 770 nm. The energy of the single pulse was of the order of 1 nJ and the pulse duration after the AOPDF was measured to be 86 fs FWHM by the autocorrelation utilizing the second harmonic generation. The shaped pulse was tightly focused into a glass cell with a singlet spherical plano-convex lens having a focal length of 400 mm, resulting in a peak intensity of 0.7 ± 0.4 GW/cm^2. The temperature of the cell was kept at 170 °C to vaporize metallic cesium. We employed the time-resolved photon counting method to detect fluorescence from the focus point as a function of time, using a multichannel scaler (Stanford Research Systems, SR430) with the dwell time of 640 ns. The fluorescence from transition (2) was measured by a photomultiplier tube (Hamamatsu, R4220P, hereafter referred by PMT1) with a 10-nm bandpass filter centered at 671.0 nm. The fluorescence from transition (3) was detected by PMT2 (Hamamatsu, R636-10) with two identical 10-nm bandpass filters centered at 694.3 nm. PMT2 also counts undesirable fluorescence from the transition

$$\mathrm{Cs}(7D_{3/2} \rightarrow 6P_{3/2}) \quad \text{at } 698.3 \text{ nm}, \qquad (5)$$

although the probability of transition (5) is about one sixth of that of transition (3). Consequently, the count rate of PMT1 should be proportional to the population in $\mathrm{Cs}(7D_{3/2})$, while that of PMT2 should be a linear combination of the populations in both $\mathrm{Cs}(7D_{5/2})$ and $\mathrm{Cs}(7D_{3/2})$.

III. RESULTS

Figure 2 shows temporal profiles of the count rate caused by a bunch of shaped pulses in two extreme cases of the delay and phase difference. Because these temporal profiles are affected by the propagation of the acoustic pulse pair, the whole area of the band structure cannot be connected with the fluorescence intensity arising from the designed pulse. Instead, only the central part of the band gives correct information on the excitation probability by the designed optical

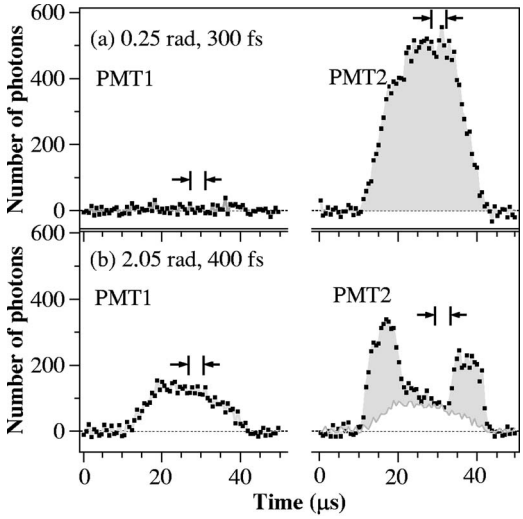

FIG. 2. Temporal profiles of the count rate from PMT1 and 2 are shown in two extreme cases of pulse shape; (a) $\delta\Phi_0=0.25$ rad and $\tau=300$ fs and (b) 2.05 rad and 400 fs. The count rate from PMT1 is proportional to the population of $Cs(7D_{3/2})$, while that from PMT2 is a linear combination of the population of $Cs(7D_{5/2})$ (filled area) and $Cs(7D_{3/2})$ (open area). The arrows indicate the timing range where the pulse shaper is correctly operated. Within this range, the contributions of $Cs(7D_{3/2})$ and $Cs(7D_{5/2})$ vanish alternately in cases (a) and (b).

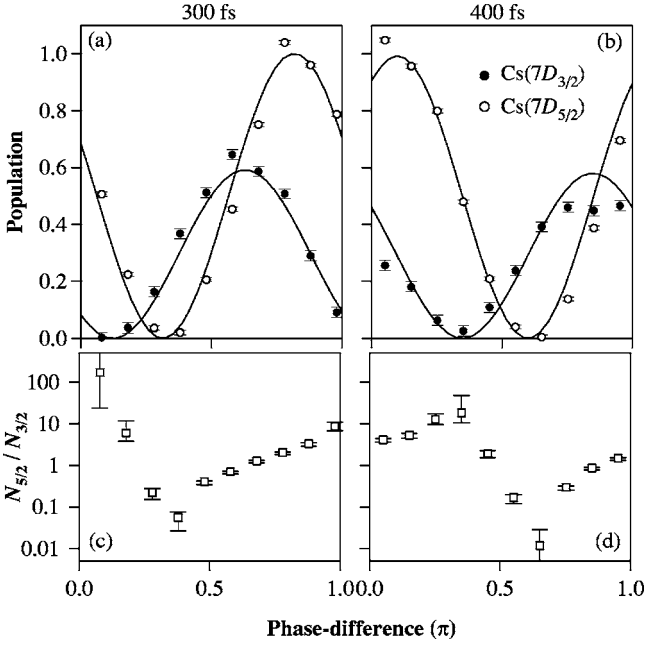

FIG. 3. Normalized populations of $Cs(7D_{3/2})$ (filled circles) and $Cs(7D_{5/2})$ (open circles) as functions of phase-difference of the pulse pair are plotted at the delay of (a) 300 fs and (b) 400 fs. Solid curves represent the results of theoretical calculation. All populations are normalized at the greater peak of the calculated populations of the two states. Lower panels, (c) and (d), show the selection ratios [the ratios of population of $Cs(7D_{5/2})$ to $Cs(7D_{3/2})$] at the respective delays. The contrast ratio of maximal to minimal selection ratio is determined as >1600 from these plots.

field. At the early (late) stage of the band, only the first (second) acoustic pulse is in the effective region of the crystal and the other pulse is out of it. Therefore, at the early or late stage, the fluorescence is induced by the optical field like a single pulse. In fact, the curve for PMT2 in Fig. 2(b) exhibits two peaks in the early and late stages. This feature can be explained by the fact that the excitation probability in the central part is suppressed by the destructive interference caused by the two optical pulses, while little interference is expected at both early and late stages due to the single-pulse character of the optical field. Note that this dual-peak feature is very small for the shorter delay as shown by the curve for PMT1 in Fig. 2(a). This observation is also consistent with the above picture. At the shorter delay, the two acoustic pulses overlap each other to the larger extent, which makes the single-pulse region (early and late stages) unclear. We have confirmed the above picture with many reproducible experiments at different delays. Therefore, we restrict the time for averaging the count rate to the range indicated by a pair of arrows in Fig. 2. We take this averaged count rate as the total fluorescence intensity arising from the designed pulse.

It is apparent that the total fluorescence intensity of both PMTs (I_1 and I_2) is drastically changed by choosing a different set of $\delta\Phi_0$ and τ as shown in Figs. 2(a) and 2(b). In particular, notice that I_1 vanishes in the case of Fig. 2(a), indicating that $Cs(7D_{3/2})$ is completely wiped out, while $Cs(7D_{5/2})$ is significantly populated as shown by I_2 in Fig. 2(a). This implies that the quantum interference, the core of the selection mechanism, is controllable with high accuracy and observable in reality.

In contrast to I_1, I_2 does not reach zero even in cases of the most destructive phase-difference, one of which is shown in Fig. 2(b). This is because I_2 contains the fluorescence from $Cs(7D_{3/2})$ via transition (5) other than that from $Cs(7D_{5/2})$. To obtain a pure contribution of $Cs(7D_{5/2})$, we subtract the contribution of transition (5) from I_2, using I_1 together with the transition dipole moments of transitions (2), (3), and (5) and their estimated detection efficiencies. The result of the subtraction is illustrated with the filled area in Fig. 2. Obviously, the pure contribution of transition (3) has vanished in the proper range of time, indicating that $Cs(7D_{5/2})$ can be completely wiped out as well as $Cs(7D_{3/2})$. As a consequence, in the two extreme cases of pulse shape, highly selective excitation has been shown for both the spin-orbit states.

To figure out the mechanism of this selection, the total fluorescence intensity was measured at various phase differences and converted to the population using the estimated detection efficiencies. As a result, we have obtained the phase difference dependence of the populations, as shown in Figs. 3(a) for the 300 fs delay and 3(b) for 400 fs. At each delay, a complete modulation is observed with a period of π, as expected from the "Ramsey fringes" in a two-photon process. The solid curves represent the results of theoretical calculations described below.

IV. CALCULATIONS

For the calculation of the population of each state, we consider the time-dependent amplitude of the wave function

in the jth electronic state of the cesium atom, $c_j(t)$, in the presence of the electric field, $E(t)$. In the electric-dipole approximation, $c_j(t)$ satisfies the coupled Schrödinger equations given by

$$i\frac{d}{dt}\begin{pmatrix} c_1(t) \\ c_2(t) \\ \vdots \end{pmatrix} = \begin{pmatrix} E_1 & -\mu_{12}E(t) & \cdots \\ -\mu_{21}E(t) & E_2 & \cdots \\ \vdots & \vdots & \ddots \end{pmatrix}\begin{pmatrix} c_1(t) \\ c_2(t) \\ \vdots \end{pmatrix}, \quad (6)$$

where E_j is the energy eigenvalue, and $\mu_{jj'}$ is the transition dipole moment. We numerically solve Eq. (6) with $j=1(6S_{1/2})$-$18(9S_{1/2})$, $c_1(-\infty)=1$, $c_{j\neq 1}(-\infty)=0$, and $E(t)$ calculated by Eq. (4) with pulse parameters appearing in the present experiment. The final populations in the $7D_J$ states are obtained by $N_J(\delta\Phi_0,\tau)=|c_j(+\infty)|^2$, where $j=16(17)$ for $J=3/2(5/2)$, as functions of $\delta\Phi_0$ and τ which are independent variables of $E(t)$. The solid curves in Figs. 3(a) and 3(b) represent the calculated $N_J(\delta\Phi_0,\tau)$, which are normalized at the greater peak calculated for the two states. In each delay, the phase-shift observed between the two excited states clearly obeys the theoretical prediction.

As a measure of the selectivity, we evaluate the contrast ratio γ defined by the ratio of the maximum to minimum of the selection ratio, $\gamma=r(\delta\Phi_0,\tau)|_{\max}/r(\delta\Phi_0,\tau)|_{\min}$, where $r(\delta\Phi_0,\tau)=N_{5/2}(\delta\Phi_0,\tau)/N_{3/2}(\delta\Phi_0,\tau)$. The measured selection ratio is plotted in Figs. 3(c) and 3(d) as a function of the phase difference. From both the maximum at $\delta\Phi_0=0.25$ rad and $\tau=300$ fs and the minimum at 2.05 rad and 400 fs, the lower limit of the contrast ratio is determined to be 1600. It is noteworthy that this high selectivity is achieved in a really short time with the delay less than 400 fs. In comparison, the state-selective excitation with a single TL pulse would require a much longer time to exhibit a similar high selectivity, e.g., the FWHM of 5.6 ps would be required when the pulse intensity has a sech^2 profile. On the other hand, a sech^2 pulse with the duration of 400 fs FWHM leads to a contrast ratio of 6.3 at most. From this viewpoint, the present selection is regarded as an ultrafast and highly precise selection.

V. DISCUSSION

The phase shifts of the excitation probability observed between the two spin-orbit states (Fig. 3) are compared to those predicted from the amplitude of the spin-orbit splitting. Blanchet and co-workers [6] showed the analytical expressions of two-photon excitation probability of transition (1) by a pulse pair in the weak field regime. According to their analysis, the final population of the $7D_J$ state is presented by

$$N_J(\delta\Phi_0,\tau) \propto 1+\cos\{(2\omega_0-\omega_J)\tau+2\delta\Phi_0\} \quad (7)$$

when the overlap between the two pulses is ignorable. Therefore, the phase-shift is noted by $\tau\Delta\omega$, i.e., 1.2 rad for $\tau=300$ fs and 1.6 rad for $\tau=400$ fs. These values are consistent with the observed phase shifts, 1.4 ± 0.2 and 1.6 ± 0.3 rad, respectively, indicating that the modulation is indeed ascribed to the quantum interference known as the "Ramsey fringes." We have also confirmed that the phase

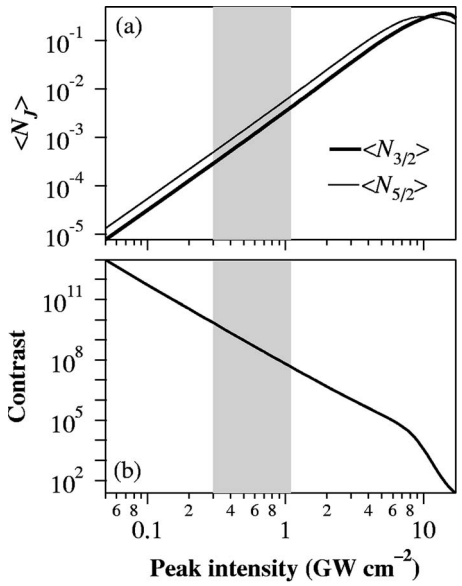

FIG. 4. Calculated intensity dependence of (a) the phase-averaged population of Cs($7D_{3/2}$) (thick line) and Cs($7D_{5/2}$) (thin line), and (b) the contrast ratio of the selection ratio at the 400-fs delay. The gray areas indicate the range of the peak intensity estimated in the experiment. From these plots, the applied intensity is proved to be in the weak field regime.

inversion occurs at much longer delay of ~800 fs as predicted by $\tau\Delta\omega=\pi$.

In the rest of this paper, we discuss the prerequisite conditions and limitations on the precise and ultrafast selection. First of all, the quantum-mechanical cancellation of the wave function must be perfect for precise selection. There are two essential conditions to satisfy this requirement. One is the coherence of the wave function in the target states. The other is the equality in amplitude of the two temporally separated wave functions. The coherence of the wave function is governed by (I) the optical coherence of pump pulse and (II) decoherent processes. The present success in precise selection implies that the optical coherence (I) can be satisfactorily pure with current technologies. The decoherent process (II) is the main theme of our future studies to extend the selection to more complicated systems. In turn, the equality in amplitude is affected by (III) decay processes and (IV) the peak intensity of the laser pulse. Although the present system is not the case, the effect of the decay processes (III) should be taken care of, e.g., for radiative decay, collisional quenching, reaction, and so on. The peak intensity (IV) must be weak to accomplish perfect cancellation in a perturbative manner. As an example, the influence of the peak intensity is theoretically examined for the present case in the next paragraph.

We calculate $N_J(\delta\Phi_0,\tau)$, varying the peak intensity of $E(t)$ in Eq. (6) and have found that until ~5 GW/cm^2 the phase-averaged population $\langle N_J\rangle$ is almost proportional to the square of the intensity [Fig. 4(a)]. This implies that below ~5 GW/cm^2 the population of the excited state is negligibly small in comparison with that of the ground state. Therefore, the present peak intensity (0.7 ± 0.4 GW/cm^2) is evidently in the weak field regime. In addition, we calculate the contrast

ratio of the selectivity to be $\sim 10^7$ at the present intensity [Fig. 4(b)]. This value is much greater than the obtained lower limit of the contrast ratio (1600), indicating that the observed high selectivity is consistent with the peak intensity despite the tight focusing and is determined by the detection limit. On the other hand, these calculations suggest that the present peak intensity is not so weak but marginally weak and that we have to care about the peak intensity in cases, such as optically-allowed one photon transition of atoms or in the use of higher power lasers.

Secondly, the limitation of the ultrafast selection is considered. The present result ($\gamma > 1600$ at $\tau\Delta\omega \sim 1.6$) might be seen violating the uncertainty principle, in which the relation, $\tau\Delta\omega > \pi$, is usually referred to. In the present mechanism, however, the selection can be unlimitedly made faster in principle, because the delay between two independent pulses can be set freely from the uncertainty limit. The drawback is the total efficiency of the excitation.

Two practical factors are important for the ultrafast selection in the present mechanism. One is the detection limit of real detecting devices. As the selection becomes faster, the total efficiency of excitation must become smaller to maintain the high selectivity. In fact, the present contrast ratio is determined by the detection limit. The other factor is the pulse duration of real laser pulses. The selection continues during the interaction time of the laser pulse with matter, so that the selection cannot be faster than the pulse duration. Although it may be hard to surmount these practical limitations, the present result demonstrates that, by utilizing quantum interference, a precise state-selection can be accomplished in a much shorter time than that derived from the relation, $\tau\Delta\omega > \pi$, only if the total efficiency of excitation is practically not important.

VI. SUMMARY

The ultrafast precise selection of two closely-lying states, $Cs(7D_J)$, was successfully demonstrated using a phase-locked pair of transform-limited pulses. The contrast ratio exceeded a thousand within 400 fs in the delay of the pulse pair, corresponding to $\tau\Delta\omega \sim 1.6$. This is the first experimental demonstration of such a precise selection in much shorter time than $\tau\Delta\omega = \pi$, indicating that the current pulse shaping technology enables the "perfect" quantum-mechanical cancellation. Although the present atomic system is too simple to be extended straightforwardly to a complicated system, the advantage of the use of broadband lasers will be highlighted for such a complicated system itself, especially for laser isotope separation. In this context, the present results encourage us to pursue the possibility of the pulse shaping technique as a powerful tool for quantum control.

ACKNOWLEDGMENTS

The authors are grateful to Professor Tajima at JAERI for his helpful discussion and to Dr. J. Koga at JAERI for his editorial help. This study was partly supported by MEXT. KAKENHI (15035220).

[1] T. Brixner, N. H. Damrauer, P. Niklaus, and G. Gerber, Nature (London) **414**, 57 (2001).
[2] S. A. Rice and M. Zhao, *Optical Control of Molecular Dynamics* (Wiley, New York, 2000).
[3] D. Goswami, Phys. Rep. **374**, 385 (2003).
[4] R. Netz, A. Nazarkin, and R. Sauerbrey, Phys. Rev. Lett. **90**, 063001 (2003).
[5] M. M. Wefers, H. Kawashima, and K. A. Nelson, J. Chem. Phys. **102**, 9133 (1995).
[6] V. Blanchet, C. Nicole, M. A. Bouchene, and B. Girard, Phys. Rev. Lett. **78**, 2716 (1997).
[7] N. F. Ramsey, *Molecular Beams* (Oxford University Press, Oxford, 1956); M. M. Salour and C. Cohen-Tannoudji, Phys. Rev. Lett. **38**, 757 (1977); R. Teets, J. Eckstein, and T. W. Hänsch, *ibid.* **38**, 760 (1977); N. F. Scherer *et al.*, J. Chem. Phys. **95**, 1487 (1991); D. W. Schumacher, J. H. Hoogenraad, D. Pinkos, and P. H. Bucksbaum, Phys. Rev. A **52**, 4719 (1995); M. Bellini, A. Bartoli, and T. W. Hänsch, Opt. Lett. **22**, 540 (1997); K. Ohmori, Y. Sato, E. E. Nikitin, and S. A. Rice, Phys. Rev. Lett. **91**, 243003 (2003).
[8] K. Yokoyama, Y. Teranishi, Y. Toya, T. Shiria, Y. Fukuda, M. Aoyama, Y. Akahane, N. Inoue, H. Ueda, K. Yamakawa, A. Yokoyama, H. Yamada, A. Yabushita, and A. Sugita, J. Chem. Phys. **120**, 9446 (2004).
[9] P. Tournois, Opt. Commun. **140**, 245 (1997); F. Verluise, V. Laude, Z. Cheng, Ch. Spielmann, and P. Tournois, Opt. Lett. **25**, 575 (2000).
[10] A. M. Weiner, Rev. Sci. Instrum. **71**, 1929 (2000).
[11] S.-H. Lee, K.-H. Jung, J. H. Sung, K.-H. Hong, and C. H. Nam, J. Chem. Phys. **117**, 9858 (2002).